Hot exciton transport in WSe_{2} monolayers

Darwin F. Cordovilla Leon, Zidong Li, Sung Woon Jang, and Parag B. Deotare

Hot exciton transport in WSe$_2$ monolayers

Darwin F. Cordovilla Leon[1,†] , Zidong Li[2,†] , Sung Woon Jang[2] and Parag B. Deotare[1, 2,‡]

[1]Applied Physics Program, University of Michigan-Ann Arbor, 450 Church St., 1425 Randall Laboratory, Ann Arbor, MI 48109, USA

[2]Electrical and Computer Engineering Department, University of Michigan-Ann Arbor, 1301 Beal Ave., Ann Arbor, MI 48109, USA

We experimentally demonstrate *hot* exciton transport in h-BN encapsulated WSe$_2$ monolayers via spatially and temporally resolved photoluminescence measurements at room temperature. We show that the nonlinear evolution of the mean squared displacement of the non-resonantly excited *hot* exciton gas is primarily due to the relaxation of its excess kinetic energy and is characterized by a density-dependent fast expansion that converges to a slower, constant rate expansion. We also observe saturation of the *hot* exciton gas' expansion rate at high excitation densities due to the balance between Auger-assisted *hot* exciton generation and the phonon-assisted *hot* exciton relaxation processes. These measurements provide insight into a process that is ubiquitous in exciton transport measurements where non-resonant optical excitation is typically employed.

[†] These authors contributed equally

[‡] Corresponding author: pdeotare@umich.edu

Exciton transport in transition metal dichalcogenide (TMD) monolayers has received significant attention[1–9] due to the prospects of TMD-based excitonic devices operating at room-temperature[6,10]. While several of these studies have focused on quantifying the transport properties of excitons in TMD monolayers[1,3,4,7,8], the origin of the apparent time-dependent exciton diffusivity observed in these materials[7,8] still remains unexplained.

Time-varying diffusivities are typically associated with anomalous diffusive transport of a distribution of particles, which is characterized by a nonlinear evolution of the distribution's mean squared displacement (MSD)[11–14]. While numerous processes in nature appear to follow anomalous diffusive behavior[15–21], the physical mechanisms that lead to such phenomena are unique to each particular system.

In layered semiconductors, the reduced Coulomb screening enhances many-body interactions, which can radically influence the dynamics of excitons, especially in the high excitation density regime[22–26]. In this work, we show that the relaxation of the kinetic energy of a *hot* gas of excitons formed by a non-resonant optical excitation and exciton-exciton Auger scattering are responsible for the nonlinear evolution of the MSD of excitons in h-BN encapsulated WSe_2 monolayers. Specifically, we explore the effect of excitation density and photon energy on the temperature of the exciton gas by monitoring the temporal evolution of the photoluminescence's (PL) spatial profile of the exciton gas at room temperature. Our results demonstrate that the initial fast expansion of the exciton gas is the result of *hot* exciton transport and has a minimal contribution from Auger broadening. Auger broadening refers to the apparent fast diffusion that results from the center of the exciton PL intensity profile dropping faster than the edges due to density dependent non-radiative Auger recombination[3].

WSe_2 monolayers were mechanically exfoliated from a bulk WSe_2 crystal and encapsulated with hexagonal boron nitride (h-BN). More details of the fabrication process can be found in the supplementary information. The PL emission of excitons in h-BN encapsulated WSe_2 monolayers was monitored using the technique described in references[7,27,28], where a temporally and spatially resolved map of the WSe_2 monolayers' PL was constructed following a pulsed laser excitation with a Gaussian intensity profile. These temporally-resolved spatial maps were built one pixel at the time by using time-correlated single photon counting while scanning an avalanche photodiode detector across the PL emission spot.

Typical optical measurements on TMD monolayers employ excitations with photon energies much higher than these materials' bandgaps. This type of excitation creates electron-hole pairs with excess energy that can be relaxed via ultrafast interaction with phonons and eventually form excitons with high center-of-mass kinetic energy and momentum[29]. Excitons with high kinetic energy have a high probability of non-radiative recombination which takes place either due to exciton dissociation, trapping by defects[29–31] or rapid exciton-exciton Auger scattering[3,24,25,31–34]. Auger scattering is much more likely to occur in systems with low dimensionality, such as WSe_2 monolayers, where the reduced Coulomb screening enhances many-body interactions[3,24,25,31–35]. Depending on the relative recombination rates, a fraction of the initially created *hot* gas completes the kinetic energy relaxation during its lifetime via exciton-phonon scattering processes[29,36]. Eventually, the relaxed or *cold* excitons recombine radiatively.

In a system of *cold* excitons moving in an energetically homogeneous medium, the MSD of a Gaussian distribution of such excitons, denoted by $\langle \Delta\sigma^2(t) \rangle$, evolves linearly with time according to $\langle \Delta\sigma^2(t) \rangle = 2Dt$, where D is the diffusion coefficient or diffusivity[37]. However, if the evolution of the MSD is nonlinear, it is typically described by the power law model $\langle \Delta\sigma^2(t) \rangle = \Gamma t^\alpha$, where Γ and α are known as the transport factor and anomalous coefficient respectively[12,14,18,38–41]. Any deviation from $\alpha = 1$ is known as anomalous diffusion[38]. Anomalous-diffusive motion of carriers and excitons has traditionally been associated with hopping transport between localized states in solids with high energetic disorder[15–19,41,42]. This type of transport is negligible in h-BN encapsulated TMD monolayers as it has been shown that encapsulation reduces energetic disorder as well as surface roughness scattering, charged impurity scattering, and exciton-exciton scattering[43–45].

Figure 1 shows the time evolution of the MSD of excitons in an h-BN encapsulated WSe_2 monolayer for increasing excitation densities. We observe a progression of the MSD evolution from linear to nonlinear as the excitation density increases. The nonlinear regime is characterized by a rapid rise of the MSD at early times, followed by a transition into a slower, constant rate expansion for timescales beyond hundreds of picoseconds. The slope the MSD at early times increases with excitation density and saturates at elevated densities. The initial exciton diffusivities range from values between 0.5 cm^2s^{-1} at low excitation and 4 cm^2s^{-1} at high excitation densities (see supplementary Figure S21). We attribute the apparent anomalous diffusive motion of excitons in h-BN encapsulated WSe_2 monolayers to the kinetic energy relaxation of *hot* excitons formed by non-resonant optical excitation[46–55] and Auger broadening.
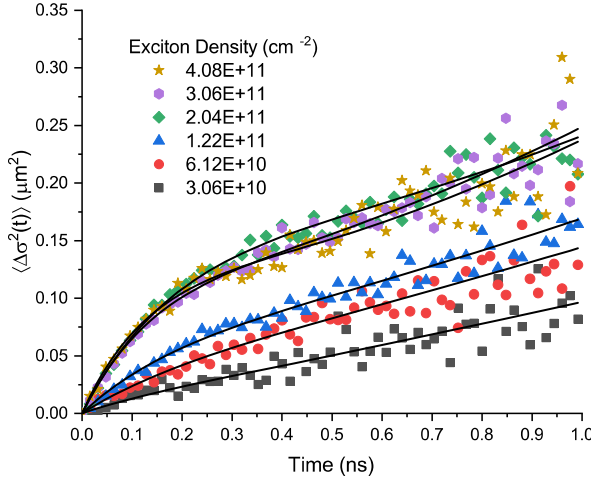

Figure 1: Evolution of the MSD of excitons in a h-BN encapsulated WSe_2 monolayer on a SiO_2/Si substrate for increasing excitation densities. The MSD is defined as $\langle\Delta\sigma^2(t)\rangle \equiv \sigma^2(t) - \sigma^2(0)$ where $\sigma(t)$ represents the standard deviation of the Gaussian distribution of excitons at time t. The solid lines represent the kinetic energy relaxation model fit represented by Eq.(3) and the markers are the experimental data. The temporally and spatially resolved maps which the MSD curves were extracted from are shown in supplementary Figures (S3)-(S12). In addition, the results of these fits are shown in supplementary Figures (S15) and (S16).

A fraction of the fast rise in MSD can be attributed to Auger broadening, which can be significant at high excitation densities[3,50,56]. In this process, the PL intensity at the center of the emission spot, where the exciton density is the highest, decreases much more rapidly than the edges due to nonradiative exciton-exciton Auger recombination[3]. Such "flattening" of the PL emission profile can be misinterpreted as spatial exciton diffusion. To quantify the contribution of Auger broadening, we analyzed the time resolved PL (TRPL) as shown in Figure 2(a). Specifically, the

evolution of the TRPL was modeled using the rate equation

$$\frac{\partial}{\partial t}n(t) = -\frac{n(t)}{\tau} - \gamma_A n^2(t) \tag{1}$$

where $n(t)$, τ and γ_A represent the exciton density, lifetime and Auger constant respectively[32]. The data in Figure 2(a) was fitted (solid lines) with the solution to this rate equation given by

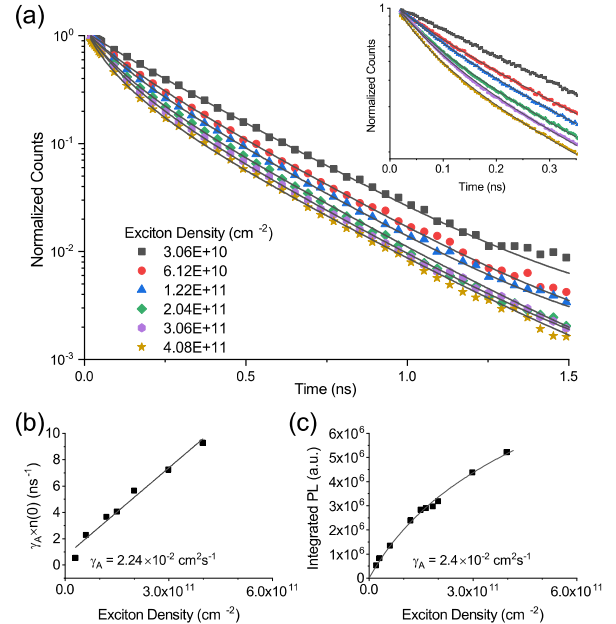$$n(t) = \frac{n(0)e^{-t/\tau}}{1 + [n(0)\gamma_A\tau](1 - e^{-t/\tau})} \tag{2}$$

Figure 2: (a) Time-resolved photoluminescence (TRPL) of a h-BN encapsulated WSe_2 monolayer transferred onto a SiO_2/Si substrate for increasing density of excitons created per optical pulse. The fits were obtained assuming 11.5% absorption of the optical excitation at 405 nm[57] and accounting for the optical losses in our measurement setup. The inset shows the PL's initial decay emphasizing the lack of excitation density-induced decay saturation. (b) Auger constant estimated by fitting the data in (a) with Eq.(2). The y-axis represents the product of the initial exciton density denoted by $n(0)$ and the Auger constant γ_A. (c) Integrated PL of the h-BN encapsulated WSe_2 monolayer for increasing density of excitons created per optical pulse. The Auger constant was estimated by fitting the PL intensity with the relation $I_{PL} \propto \ln[1 + n(0)\gamma_A\tau](\gamma_A\tau)^{-1}$[3]. The solid lines indicate the fits, and the markers the experimental data.

Our excitation density range falls within the mid excitation density regime according to other density-dependent studies on this material[3]. The estimated values for Auger constant and exciton lifetime from our TRPL measurements are 0.02 cm^2s^{-1} and 0.23 ns respectively as shown in Figure 2(b-c). Based on these values, the contribution of Auger broadening to the

MSD should be minimal for excitation densities below $2 \quad$ cm^{-2} (i.e. $\quad$). To confirm this prediction, the Auger constant obtained in Figure 2 was used to estimate the degree of Auger broadening in our measurements at various excitation densities and found very little contribution to the total MSD for excitation densities below $4 \quad$ cm^{-2} (see supplementary Figure S2). This observation is consistent with other reports where exciton-exciton Auger scattering has been shown to be drastically reduced in h-BN encapsulated TMD monolayers[45]. More importantly, Auger broadening cannot explain the saturation observed in Figure 1 at excitation densities above $2 \quad$ cm^{-2} as the integrated PL intensity continues to rise for excitation densities above this value as shown in Figure 2(c). Furthermore, the Auger coefficient extracted from the integrated PL intensity using the relation $\quad$ from reference[3] is consistent with the Auger coefficient obtained from our TRPL measurements. Therefore, the fast rise of the MSD at early times is caused predominantly by the fast motion of *hot* excitons whose average temperature is higher than the lattice temperature[48,50,51,53,58]. Consequently, the progression from fast to slow evolution of the MSD for a given excitation density can be explained as the transition from a *hot* gas of excitons, which move very fast due to their high kinetic energy, to a *cold* gas of excitons that move more slowly after having relaxed their excess kinetic energy. While dark excitons are known to play a major role in WSe$_2$'s PL, this contribution should remain constant over our excitation density regime.

The formation of *hot* excitons is possible by non-resonant excitation into the continuum of states. Following non-resonant excitation, the *hot* carriers could relax down to the bottom of the continuum via carrier-phonon scattering and form excitons with zero center-of-mass momentum. However, the direct formation of *hot* excitons via scattering with optical phonons shortly after non-resonant excitation is another possibility. In principle, these two exciton formation channels are both possible, and the dominant mechanism depends on their relative rates and on the material system. For instance, in III-V semiconductors, where excitons have low binding energies, the electrons and holes may relax towards their band minima individually and form excitons after the energy relaxation process[53]. On the other hand, in materials with much larger exciton binding energies, the formation of *hot* excitons via phonon scattering is much more efficient process, thus dominating over the individual relaxation of electrons and holes[53]. Since it has been shown that excitons in TMD monolayers form in ultrafast timescales due to their large binding energies[57,59] and presence of optical phonons, the direct formation of *hot* excitons following non-resonant

optical excitation is most likely the more efficient mechanism in these materials.

The distribution of kinetic energy immediately after the formation of *hot* excitons is very far from equilibrium. This distribution evolves towards quasi-equilibrium described by an effective temperature via scattering with other *hot* excitons and with phonons[29]. After a thermalized distribution is achieved, and before recombination occurs, *hot* excitons typically lose their excess kinetic energy to the lattice via phonon scattering[29]. In the high excitation density regime, however, the cooling of *hot* excitons by exciton-phonon scattering is counteracted by the heating of the exciton gas via exciton-exciton Auger scattering[46,47]. During this Auger process, an exciton recombines non-radiatively and transfers its energy to a nearby exciton which ionizes into *hot* carriers with excess energy of the order of the bandgap energy. These *hot* carriers lose their excess energy again via carrier-phonon and carrier-carrier scattering and eventually form new excitons with kinetic energies that may be higher than the originally-formed excitons' kinetic energy. These newly-formed *hotter* excitons then scatter with the remaining colder excitons thereby increasing the overall gas temperature[46]. A schematic illustration of the exciton formation and Auger heating processes, as well as a timescale of the exciton formation, relaxation and transport regimes are shown in Figure 3.
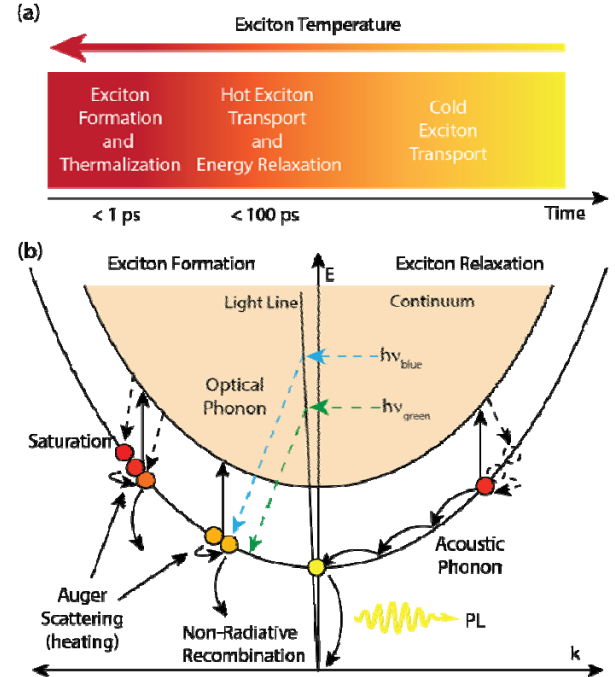

Figure 3: Schematic diagram illustrating (a) the timescales of exciton formation, *hot* and *cold* exciton transport regimes as well as the evolution of the temperature of the exciton gas, and (b) exciton dispersion relation showing the exciton formation and relaxation processes. The saturation refers to

the rate balance between exciton-exciton Auger scattering and exciton-phonon scattering.

Auger heating depends strongly on the density of the exciton population, which implies that it is most likely to occur early in the relaxation process when the density of the exciton gas is at its highest. While *hot* excitons relax their kinetic energy, they can also propagate and while doing so their speed should decrease. After the exciton density has decayed enough for Auger scattering to become less relevant, and the excess kinetic energy of the exciton gas has been relaxed to the lattice via exciton-phonon scattering, the remaining *cold* excitons diffuse at a constant rate. This trend is consistent with our observations of the nonlinear evolution of the MSD of h-BN encapsulated WSe$_2$ monolayers shown in Figure 1.

The evolution of the MSD of a gas of excitons created by an optical pulse with a Gaussian spatial profile can be modeled as $\langle \Delta\sigma^2(t) \rangle = 2tD(t)$, where the time-varying diffusivity $D(t)$ depends on the instantaneous effective temperature of the exciton gas $T(t)$[55]. While the mobilities and diffusivities of the individual electron and hole making up an exciton are not necessarily identical, by assuming that they are, an explicit form of the exciton diffusivity could be written using the Einstein relation as $D(t) = \mu_q k_B T(t)/q$ where μ_q represents the mobility of a carrier with charge q, and k_B is the Boltzmann constant. Since the energy of the exciton gas is relaxed to the lattice via phonon scattering, the evolution of the exciton temperature could be modeled as $T(t) = T_0 + T^* e^{-t/\tau^*}$ where T_0, T^* and τ^* represent the exciton gas steady-state temperature, the initial excess temperature, and the kinetic energy relaxation time constant respectively. If the exciton gas completely relaxes its excess kinetic energy before it recombines, the steady-state temperature should equal the lattice temperature, and the kinetic energy relaxation time constant is approximately equal to the lifetime. With these definitions, the instantaneous exciton diffusivity could be rewritten as

$$D(t) = \frac{\mu_q k_B}{q} T(t) = D_0 + D^* e^{-t/\tau^*} \qquad (3)$$

Where similarly D_0 and D^* represent the steady-state and excess exciton diffusivity respectively. The fast initial evolution rate of the MSD is therefore proportional to the value of the instantaneous diffusivity in the limit as time approaches zero, i.e. $\lim_{t\to 0}[d\langle\Delta\sigma^2(t)\rangle/dt] = \lim_{t\to 0}[2tD(t)] = 2[D_0 + D^*]$. Equation (3) was used to fit the MSD of the exciton gas in a h-BN encapsulated WSe$_2$ monolayer and the resulting excess diffusivities are shown in Figure 4. Following the same trend as the slope of the MSD, the fitted excess diffusivity D^* appears to increase as the excitation density increases, and it also saturates at elevated excitation densities. This saturation is expected to occur due to the balancing effects of Auger heating and phonon cooling of the exciton gas discussed earlier. It is well known that the carrier or exciton-phonon scattering rate increases as the energy of the carrier or exciton increases[60]. This implies that exciton-phonon scattering is more likely to dominate the energy transfer mechanism that determines the temperature of the exciton gas at high excitation densities. Therefore, the observed saturation of the initial slope of the MSD and the extracted initial excess diffusivity, which is proportional to the gas temperature, is consistent with the balance between exciton-phonon scattering, which removes energy from the exciton gas, and Auger heating, which increases the energy of the exciton gas. In addition, in supplementary Figure (S22) we estimated the time-averaged velocity at which the measured PL spot corresponding to Figure 1 broadens and compared it to experimental carrier saturation velocities determined by electrical measurements[61]. We found that the velocity at which we observed saturation of the MSD's initial slope is about two orders of magnitude below the saturation velocity of electrons and holes in WSe$_2$. The result further confirms that *hot* excitons and not individual *hot* carriers are the responsible mechanisms for the trends observed in the experiments.

To further confirm our conclusion, we performed an experiment on a different h-BN encapsulated WSe$_2$ monolayer with lower excitation photon energy. If the nonlinear evolution of the MSD is indeed caused by the relaxation of kinetic energy of a *hot* exciton gas and not Auger broadening, then for lower excitation energies, the saturation of the initially-fast MSD slope and initial excess exciton diffusivity and temperature should occur at higher excitation densities. This is expected because the higher the excitation energy, the higher the kinetic energy of the initially formed *hot* exciton gas, and the less energy that will be required via Auger heating to reach the saturation temperature. This trend is precisely evidenced in Figure 4 where the excess diffusivity of the initially formed exciton gas is shown for two different excitation energies, 3.1 eV (405 nm) and 2.4 eV (520 nm), and increasing excitation densities.
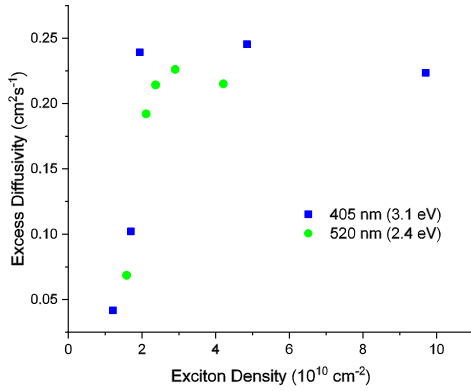
Figure 4: Excess diffusivity of excitons in a h-BN encapsulated WSe_2 monolayer created by two lasers with different photon energies and increasing excitation densities obtained by fitting the MSD with the model $\langle \Delta \sigma^2(t) \rangle = 2tD(t) = 2t[D_0 + D^* e^{-t/\tau}]$, where the steady state diffusivity was assumed to be $D_0 = \mu_q k_B T_0 / q$ with T_0 set to the lattice temperature at 300 K. The saturation of the excess diffusivity and corresponding excess temperature of the exciton gas occurs at a higher excitation density for the optical excitation with lower photon energy (2.4 eV) than for the optical excitation with higher photon energy (3.1 eV). The data correspond to a sample that is different from that shown in Figure 1. Further details of these fits can be found in supplementary Figures (S17)-(S20).

As expected, the excitation density required to reach the saturation excess diffusivity with the lower photon energy excitation (520 nm) is higher than the excitation density required to reach the same saturation diffusivity with the higher photon energy excitation (405 nm). This correlation between excitation density and photon energy is convincing evidence that the initial fast motion of the exciton gas stems primarily from the motion of *hot* excitons created by non-resonant excitation rather than Auger broadening.

In summary, through a systematic investigation via temporally and spatially resolved PL measurements at room temperature, we have determined the origin of the apparently anomalous diffusive motion of excitons in h-BN encapsulated WSe_2 monolayers. Specifically, we have shown that the nonlinear evolution of the MSD of an exciton gas in a h-BN encapsulated WSe_2 monolayer created by a high-density, non-resonant optical excitation is dominated by *hot* exciton transport. We observed a correlation between the initial slope of the MSD and the excitation density that saturates at elevated excitation densities. This saturation is consistent with the balancing effects of Auger heating and phonon cooling that respectively increase and decrease the temperature of the exciton gas. We confirmed that the excitation density required to reach the saturation excess diffusivity depends on the excitation's photon energy. That is, a higher photon energy excitation requires a lower excitation density to reach the saturation excess diffusivity. These results offer new insight into a process that is ubiquitous in exciton transport dynamics in TMDs where high-density, non-resonant optical excitation is typically employed and will aid in the design of excitonic devices that exploit the regimes of *hot* and *cold* exciton transport.

See supplementary material for details of the fabrication processes, and data analysis.

REFERENCES

[1] F. Cadiz, C. Robert, E. Courtade, M. Manca, L. Martinelli, T. Taniguchi, K. Watanabe, T. Amand, A.C.H. Rowe, D. Paget, B. Urbaszek, and X. Marie, Appl. Phys. Lett. **112**, 152106 (2018).

[2] A. Ghazaryan, M. Hafezi, and P. Ghaemi, Phys. Rev. B **97**, 245411 (2018).

[3] M. Kulig, J. Zipfel, P. Nagler, S. Blanter, C. Schüller, T. Korn, N. Paradiso, M.M. Glazov, and A. Chernikov, Phys. Rev. Lett. **120**, 207401 (2018).

[4] N. Kumar, Q. Cui, F. Ceballos, D. He, Y. Wang, and H. Zhao, Nanoscale **6**, 4915 (2014).

[5] T. Kato and T. Kaneko, ACS Nano **10**, 9687 (2016).

[6] D. Unuchek, A. Ciarrocchi, A. Avsar, K. Watanabe, T. Taniguchi, and A. Kis, Nature **560**, 340 (2018).

[7] D.F. Cordovilla Leon, Z. Li, S.W. Jang, C.-H. Cheng, and P.B. Deotare, Appl. Phys. Lett. **113**, 252101 (2018).

[8] Z. Li, D. Cordovilla Leon, S.W. Jang, and P. Deotare, Bull. Am. Phys. Soc. (2019).

[9] K. Wang, K. De Greve, L.A. Jauregui, A. Sushko, A. High, Y. Zhou, G. Scuri, T. Taniguchi, K. Watanabe, M.D. Lukin, H. Park, and P. Kim, Nat. Nanotechnol. **13**, 128 (2018).

[10] L.V. V Butov, Superlattices Microstruct. **108**, 2 (2017).

[11] R. Metzler and J. Klafter, Phys. Rep. **339**, 1 (2000).

[12] S. Havlin and D. Ben-Avraham, Adv. Phys. **36**, 695

(1987).

[13] A. Piryatinska, A.I. Saichev, and W.A. Woyczynski, Phys. A Stat. Mech. Its Appl. **349**, 375 (2005).

[14] J.-P. Bouchaud and A. Georges, Phys. Rep. **195**, 127 (1990).

[15] G. Pfister and H. Scher, Adv. Phys. **27**, 747 (1978).

[16] G. Pfister and H. Scher, Phys. Rev. B **15**, 2062 (1977).

[17] H. Scher and E.W. Montroll, Phys. Rev. B **12**, 2455 (1975).

[18] S.M. Vlaming, V.A. Malyshev, A. Eisfeld, and J. Knoester, J. Chem. Phys. **138**, 214316 (2013).

[19] B. Movaghar, M. Grünewald, B. Ries, H. Bassler, and D. Würtz, Phys. Rev. B **33**, 5545 (1986).

[20] K. Ritchie, X.-Y. Shan, J. Kondo, K. Iwasawa, T. Fujiwara, and A. Kusumi, Biophys. J. **88**, 2266 (2005).

[21] B. Ayala-Orozco, G. Cocho, H. Larralde, G. Ramos-Fernandez, J.L. Mateos, and O. Miramontes, Behav. Ecol. Sociobiol. **55**, 223 (2004).

[22] G. Wang, A. Chernikov, M.M. Glazov, T.F. Heinz, X. Marie, T. Amand, and B. Urbaszek, Rev. Mod. Phys. **90**, 021001 (2018).

[23] D.Y. Qiu, F.H. Da Jornada, and S.G. Louie, (2013).

[24] N. Kumar, Q. Cui, F. Ceballos, D. He, Y. Wang, and H. Zhao, Phys. Rev. B **89**, 125427 (2014).

[25] S. Mouri, Y. Miyauchi, M. Toh, W. Zhao, G. Eda, and K. Matsuda, Phys. Rev. B **90**, 155449 (2014).

[26] A. Rustagi and A.F. Kemper, Nano Lett. **18**, 455 (2018).

[27] P.B. Deotare, W. Chang, E. Hontz, D.N. Congreve, L. Shi, P.D. Reusswig, B. Modtland, M.E. Bahlke, C.K. Lee, A.P. Willard, V. Bulović, T. Van Voorhis, and M.A. Baldo, Nat. Mater. **14**, 1130 (2015).

[28] G.M. Akselrod, P.B. Deotare, N.J. Thompson, J. Lee, W.A. Tisdale, M.A. Baldo, V.M. Menon, and V. Bulović, Nat. Commun. **5**, 3646 (2014).

[29] S. Permogorov, *Hot Excitons in Semiconductors* (1975).

[30] H. Wang, C. Zhang, and F. Rana, Nano Lett. **15**, 339 (2015).

[31] H. Wang, J.H. Strait, C. Zhang, W. Chan, C. Manolatou, S. Tiwari, and F. Rana, Phys. Rev. B **91**, 165411 (2015).

[32] L. Yuan, T. Wang, T. Zhu, M. Zhou, and L. Huang, J. Phys. Chem. Lett. **8**, 3371 (2017).

[33] Y. Yu, Y. Yu, C. Xu, A. Barrette, K. Gundogdu, and L. Cao, Phys. Rev. B **93**, 201111 (2016).

[34] X. Li, M.L. Tang, Y. Xu, Q. Wang, K. Liu, J.-W. Chen, J.-J. Cao, C. Zhang, H. Fu, H.-L. Zhang, X.Y. Zhu, M.L. Steigerwald, M.Y. Sfeir, and L.M. Campos, Chem. Commun. **53**, 4429 (2017).

[35] D. Sun, Y. Rao, G.A. Reider, G. Chen, Y. You, L. Brézin, A.R. Harutyunyan, and T.F. Heinz, Nano Lett. **14**, 5625 (2014).

[36] S. Brem, M. Selig, G. Berghaeuser, and E. Malic, Sci. Rep. **8**, 8238 (2018).

[37] J.-P. Bouchaud and A. Georges, Phys. Rep. **195**, 127 (1990).

[38] J. Wu and K.M. Berland, Biophys. J. **95**, 2049 (2008).

[39] G. Zumofen, J. Klafter, and A. Blumen, J. Stat. Phys. **65**, 991 (1991).

[40] R. Metzler and J. Klafter, J. Phys. A. Math. Gen. **37**, R161 (2004).

[41] G.M. Akselrod, F. Prins, L. V. Poulikakos, E.M.Y. Lee, M.C. Weidman, A.J. Mork, A.P. Willard, V. Bulović, and W.A. Tisdale, Nano Lett. **14**, 3556 (2014).

[42] R. Schwarz, J. Non. Cryst. Solids **227–230**, 148 (1998).

[43] C.R. Dean, A.F. Young, I. Meric, C. Lee, L. Wang, S. Sorgenfrei, K. Watanabe, T. Taniguchi, P. Kim, K.L. Shepard, and J. Hone, Nat. Nanotechnol. **5**, 722 (2010).

[44] F. Cadiz, E. Courtade, C. Robert, G. Wang, Y. Shen, H. Cai, T. Taniguchi, K. Watanabe, H. Carrere, D. Lagarde, M. Manca, T. Amand, P. Renucci, S. Tongay, X. Marie, and B. Urbaszek, Phys. Rev. X **7**, 021026 (2017).

[45] Y. Hoshi, T. Kuroda, M. Okada, R. Moriya, S. Masubuchi, K. Watanabe, T. Taniguchi, R. Kitaura, and T. Machida, Phys. Rev. B **95**, 241403 (2017).

[46] G.M. Kavoulakis, G. Baym, and J.P. Wolfe, Phys. Rev. B **53**, (1996).

[47] K.E. O'hara, J.R. Gullingsrud, and J.P. Wolfe, Phys. Rev. B **60**, (1999).

[48] B. Dal Don, H. Zhao, G. Schwartz, and H. Kalt, Phys. Status Solidi Basic Res. **241**, 579 (2004).

[49] H. Zhao, S. Moehl, and H. Kalt, Appl. Phys. Lett. **81**, 2794 (2002).

[50] H.W. Yoon, D.R. Wake, J.P. Wolfe, and H. Morkog, Phys. Rev. B **46**, 13 462 (1992).

[51] H. Zhao, B. Dal Don, G. Schwartz, and H. Kalt, Phys. Rev. Lett. **94**, (2005).

[52] K.E. O'Hara and J.P. Wolfe, Phys. Rev. B - Condens. Matter Mater. Phys. **62**, 12909 (2000).

[53] H. Zhao and H. Kalt, in *Opt. Semicond. Their Nanostructures* (Springer, 2004), pp. 19–45.

[54] H. Zhao, B. Dal Don, S. Moehl, and H. Kalt, Phys. Status Solidi Basic Res. **238**, 529 (2003).

[55] E. Najafi, V. Ivanov, A. Zewail, and M. Bernardi, Nat. Commun. **8**, 15177 (2017).

[56] J. Warren, K. O'Hara, and J. Wolfe, Phys. Rev. B - Condens. Matter Mater. Phys. **61**, 8215 (2000).

[57] P. Steinleitner, P. Merkl, P. Nagler, J. Mornhinweg, C. Schüller, T. Korn, A. Chernikov, and R. Huber, Nano Lett. **17**, 1455 (2017).

[58] H. Zhao, B. Dal Don, S. Moehl, H. Kalt, K. Ohkawa, and D. Hommel, Phys. Rev. B - Condens. Matter Mater. Phys. **67**, (2003).

[59] F. Ceballos, Q. Cui, M.Z. Bellus, and H. Zhao, Nanoscale **8**, 11681 (2016).

[60] B.K. Ridley, *Quantum Processes in Semiconductors*, 4th ed. (Oxford University Press, 1999).

[61] Z. Jin, X. Li, J.T. Mullen, and K.W. Kim, Phys. Rev. B - Condens. Matter Mater. Phys. **90**, 045422 (2014).